

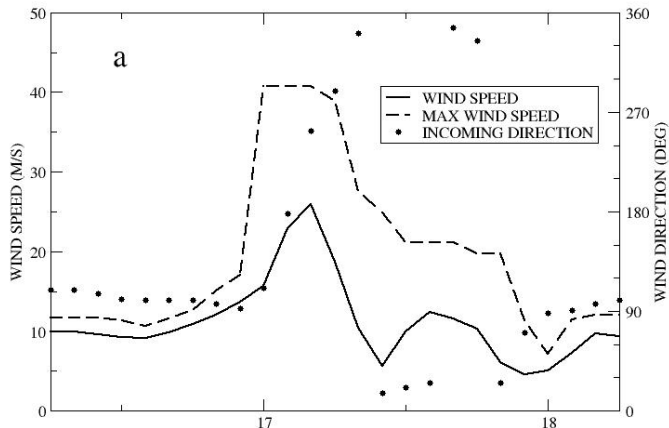
# Modelling the Impact of Squall on Wind Waves

Victor Shrira & Sergei Annenkov

Department of Mathematics,  
Keele University, UK

1st International Workshop on Waves, Storm Surges and Coastal Hazards,  
Liverpool, September 10-15, 2017

# What is squall?



An example of time history of the five minutes mean and maximum wind speeds and related directions during consecutive five minute records at the ISMAR oceanographic tower (from Cavaleri (2012))

## Motivation

- ▶ From meteorologist perspective squalls are too small scale and, therefore, difficult to predict, which makes them particularly dangerous. **What could we say about effect of squall on waves?**
- ▶ It is accepted wisdom that we can model and hence predict evolution of wind wave spectra employing the kinetic (KE), aka Hasselmann equation. To what extent it is true for rapidly varying conditions (e.g. sharp change of wind) is not known, since the KE is derived under assumption of "quasi-stationary" environment.
- ▶ For rogue waves prediction, it is essential to predict the probability density function (PDF) of surface elevations, not just the spectrum.

# What will we do?

- ▶ Simulate wave spectra under squall employing both the KE (which is not supposed to work for the squall) and GKE (which does not employ quasi-stationarity assumption).
- ▶ Examine evolution of higher moments and the PDF of surface elevation

# Statistical description. KE & Generalized KE (GKE)

**KE:**

$$\frac{dn(\mathbf{k}, \mathbf{x}, t)}{dt} = S_{input} + S_{diss} + S_{nl}$$

where ,  $n(\mathbf{k}$  is the 2D wave action spectrum.

$$S_{nl} = 4\pi \int T_{0123}^2 f_{0123} \delta_{0+1-2-3} \delta(\omega_0 + \omega_1 - \omega_2 - \omega_3) d\mathbf{k}_{123},$$

where  $f_{0123} = n_2 n_3 (n_0 + n_1) - n_0 n_1 (n_2 + n_3)$ ,

$n_i \equiv n(\mathbf{k}_i)$ ,  $\delta_{0+1-2-3} \equiv \delta(\mathbf{k}_0 + \mathbf{k}_1 - \mathbf{k}_2 - \mathbf{k}_3)$

**GKE:**

$$\frac{\partial n_0}{\partial t} = 4Re \int T_{0123}^2 \left[ \int_0^t e^{-i\Delta\omega(\tau-t)} f_{0123} d\tau \right] \delta_{0+1-2-3} d\mathbf{k}_{123} \\ + 2Re \int \left[ iT_{0123} J_{0123}^{(1)}(0) e^{i\Delta\omega t} \right] \delta_{0+1-2-3} d\mathbf{k}_{123}.$$

# Simulations of the GKE

The numerical grid is  $101 \times 31$ ,  $\omega \times \theta$ .  $\omega$  varies in the interval  $0.5, 3$  with logarithmic spacing. Angle  $\theta$  is between  $-2\pi/3$  and  $2\pi/3$ . The initial peak is at  $\omega = 1$  and angle  $\theta = 0$ . The scaling is such  $g = 1$ , so that  $k = 1$  at the peak. For the Hasselmann equation the grid is exactly the same.

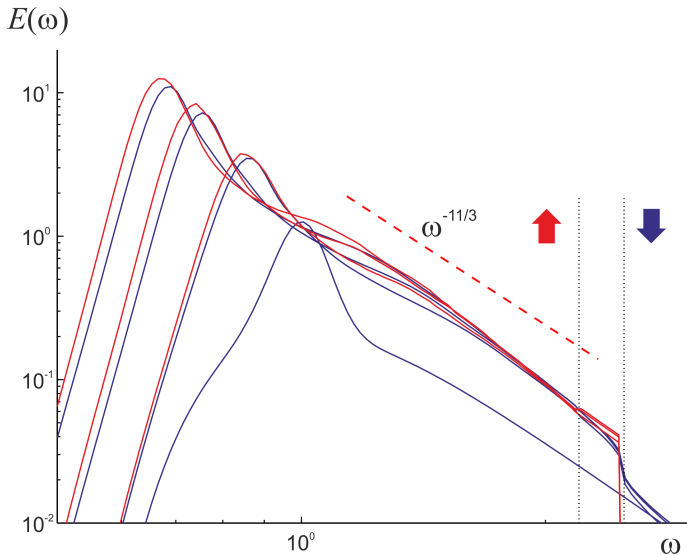
**Initial conditions:** Donelan et al (1985) with  $2 \leq U/c \leq 7.5$ ,  $\omega_p = 1$ .

**Wind forcing:** Hsiao & Shemdin (1985), characterized by initial  $U/c_p$ .

Runge-Kutta-Fehlberg with automatic step choice (step  $\leq 1/3$  of the period). After each step, all the previous history is stored, so there is no integration over the past. **The Hasselmann collision integral is computed using the code kindly provided by Gerbrant van Vledder (Delft University of Technology).**

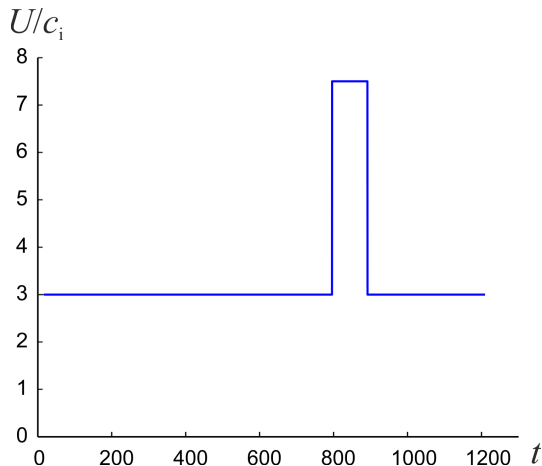
In the GKE the number of interactions is due to chosen  $\Delta\omega/\omega_{min} = 0.25$  is very large (the total number is  $\approx 3 \cdot 10^9$ ).

# Simulations $E(\omega)$ : GKE vs Hasselmann



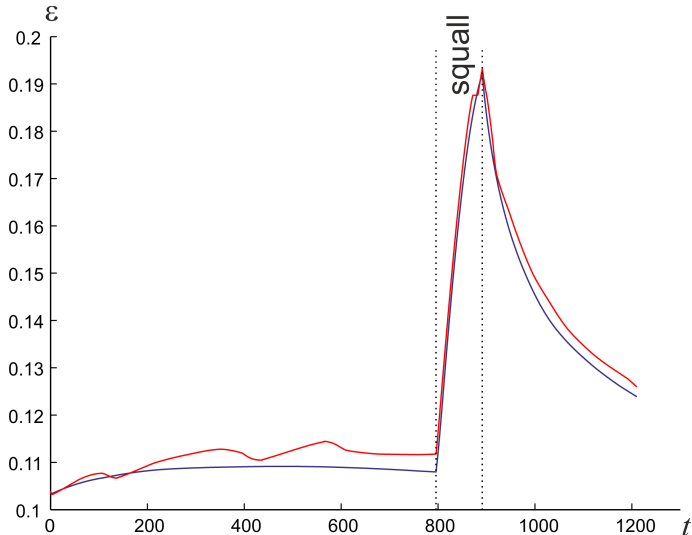
—the GKE simulations      —the Hasselmann simulations. Spectra are plotted every 160 characteristic periods

# Squall

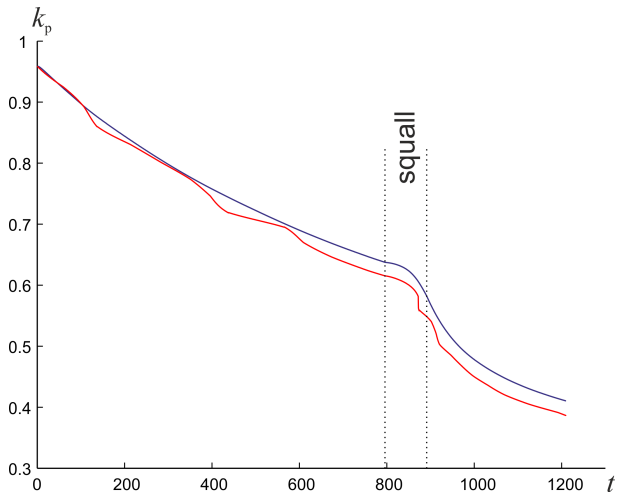


Wind speed as function of time for the squall. Wind is normalized by the phase speed of the spectral peak of the initial condition, time is measured in periods of the spectral peak of the initial condition.

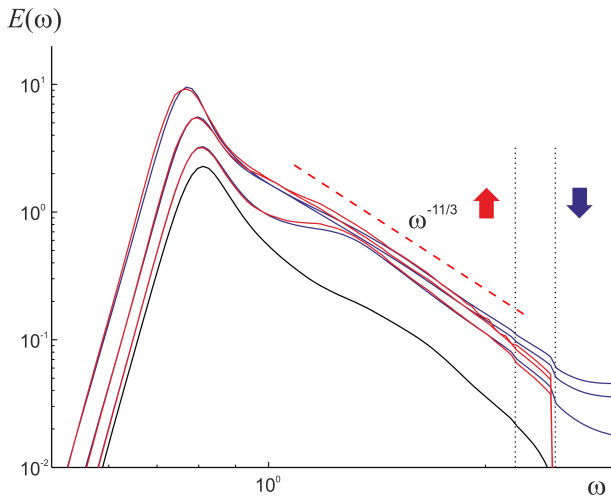
# Evolution of wave steepness



Evolution of wave steepness during the squall, with the same colour code.

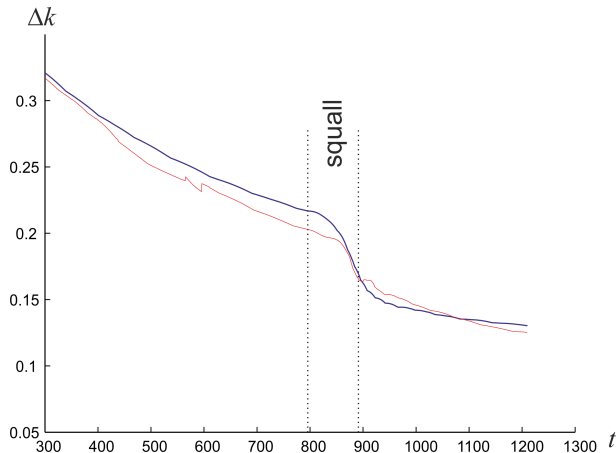


Evolution of wavenumber of the spectral peak for the squall, with the GKE and the Hasselmann equation



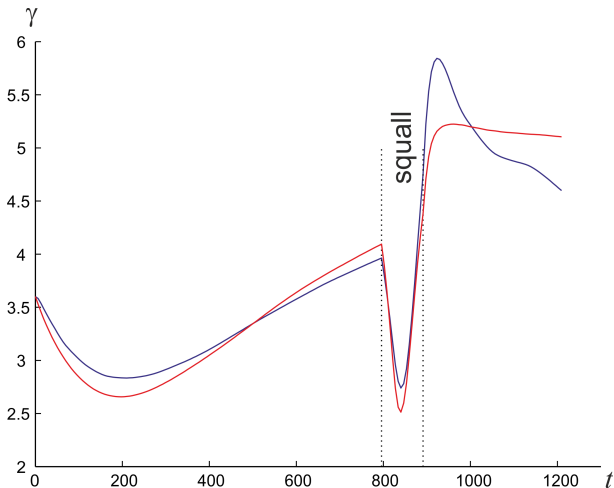
Comparison of the GKE and Hasselmann equation solutions during the squall. In this case, for a direct comparison, initial condition for the Hasselmann equation is taken as the GKE spectrum at the beginning of the squall

# Evolution of spectral width



Evolution of spectral width (taken as the width of the one-dimensional spectrum at half amplitude of the peak), with the (GKE —blue) and the Hasselmann equation (—red)

# Evolution of peakedness $\gamma$



Evolution of the fitted JONSWAP parameter  $\gamma$

## PDF of surface elevations

PDF for wave heights can be expressed in terms of the third and fourth moments (Janssen 2014)

$$p(h) = 4he^{-2h^2} \left\{ 1 + \frac{\kappa_4}{3}(2h^4 - 4h^2 + 1) + \frac{\kappa_3}{72}(4h^6 - 18h^4 + 18h^2 - 3) \right\}$$

Here  $\kappa_4 = \kappa_{40} + \kappa_{04} + 2\kappa_{22}$ ,

$$\kappa_3^2 = 5(\kappa_{30}^2 + \kappa_{03}^2) + 9(\kappa_{21}^2 + \kappa_{12}^2) + 6(\kappa_{30}\kappa_{12} + \kappa_{03}\kappa_{21})$$

$$\kappa_{mn} = \frac{\langle \eta^m \zeta^n \rangle}{\langle \eta^2 \rangle^{m/2} \langle \zeta^2 \rangle^{n/2}}$$

$\eta$  is surface elevation,  $\zeta$  is its Hilbert transform.

Thus, to find PDF we first have to examine evolution of the moments.

## Higher moments

There are two qualitatively different contributions due to non-Gaussianity to the fourth-order correlators. The first, characterised by dynamical kurtosis  $C_4^{(d)}$ , is due to quartet interactions of free waves

$$C_4^{(d)} = m_4/m_2^2 - 3, \quad m_2 = \int \omega_0 n_0 d\mathbf{k}_0, \quad m_4 = \langle \eta^4 \rangle$$

This fourth moment of the surface elevation  $\eta$  due to wave interactions is expressed through the quantity  $\text{Re} J_{0123}^{(1)}$  we compute simulating the GKE

$$m_4 = \langle \eta^4 \rangle = \frac{3}{2} \text{Re} \int (\omega_0 \omega_1 \omega_2 \omega_3)^{1/2} J_{0123}^{(1)} d\mathbf{k}_{0123}$$

All resonant and non-resonant interactions contribute to kurtosis, while the spectral evolution depends only on the near-resonant interactions.

$C_4^{(d)}$ 

If the spectral evolution is slow, we can calculate the kurtosis  $C_4^{(d)}$  from the spectrum (Janssen 2003)

$$C_4^{(d)} \approx \frac{3}{2m_2^2} \int T_{0123} (\omega_0 \omega_1 \omega_2 \omega_3)^{1/2} \frac{\cos(\Delta\omega t) - 1}{\Delta\omega} f_{0123} \delta_{0+}$$

where  $\Delta\omega = \omega_0 + \omega_1 - \omega_2 - \omega_3$ , or, in the large time limit

$$C_4^{(d)} \approx -\frac{3}{2m_2^2} \int T_{0123} (\omega_0 \omega_1 \omega_2 \omega_3)^{1/2} \frac{f_{0123}}{\Delta\omega} \delta_{0+1-2-3} d\mathbf{k}_{0123}$$

(Cauchy principal value of the integral is taken.)

If the evolution is not slow we use more lengthy nonlocal formulae

Higher moments calculated for empirical spectra: Annenkov & Shrira, J. Phys.

Oceanogr. **44**, 1582–1594 (2014).

## Bound harmonics non-gaussianity

The second component of non-gaussianity is due to bound harmonics, and can be calculated from the spectrum, if the dynamic non-gaussianity is small (the dynamic kurtosis  $C_4^{(d)} \ll 1$ ). Second moment

$$\begin{aligned}\mu_2 = \langle \eta^2 \rangle &= \int \omega_0 n_0 \, d\mathbf{k}_0 + \int (\mathcal{A}_{0,1}^2 + \mathcal{B}_{0,1}^2 + 2\mathcal{C}_{0,0,1,1}) \omega_0 \omega_1 n_0 n_1 \, d\mathbf{k}_{01} \\ &= \int \omega_0 n_0 \, d\mathbf{k}_0\end{aligned}$$

The right integral cancels due to symmetry. Third moment

$$\mu_3 = \langle \eta^3 \rangle = 3 \int (\mathcal{A}_{0,1} + \mathcal{B}_{0,1}) \omega_0 \omega_1 n_0 n_1 \, d\mathbf{k}_{01}$$

Fourth moment

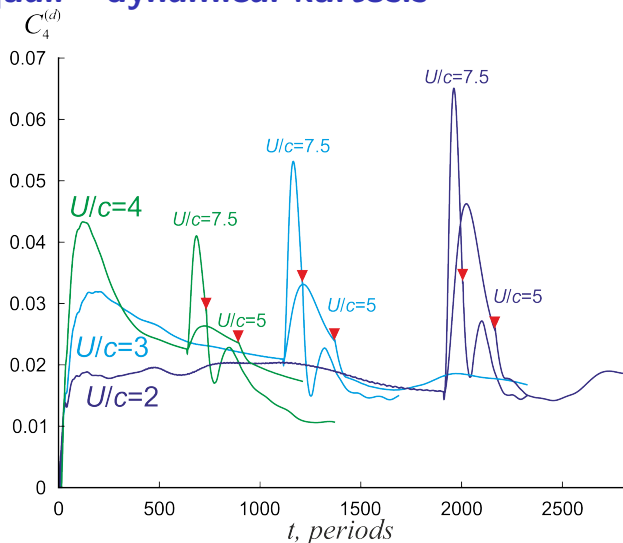
$$\mu_4 = 3 \int \omega_0 \omega_1 n_0 n_1 \, d\mathbf{k}_{01} + 12 \int \mathcal{J}_{012}^{(4)} \omega_0 \omega_1 \omega_2 n_0 n_1 n_2 \, d\mathbf{k}_{012}$$

Then, the bound harmonic components of skewness and kurtosis are

$$C_3^{(b)} = \frac{\mu_3}{\mu_2^{3/2}}, \quad C_4^{(b)} = \frac{\mu_4}{\mu_2^2} - 3.$$

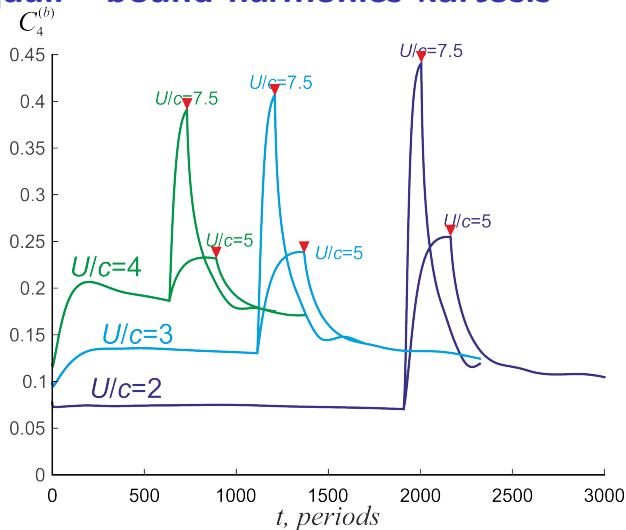
Coefficients were derived by P.Janssen (2009).

# Squall - dynamical kurtosis



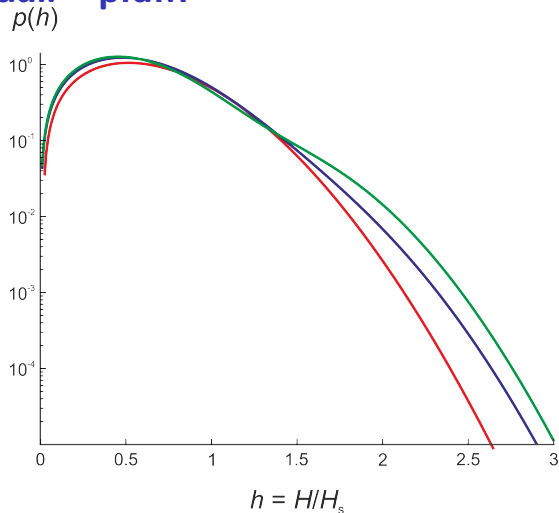
Evolution of the dynamical kurtosis  $C_4^{(d)}$ , initially under constant wind forcing with initial  $U/c_p = 2, 3, 4$ , then instantly increasing to 5 or 7.5 and decreasing back to the initial value. Red triangles mark end of squall

# Squall - bound harmonics kurtosis



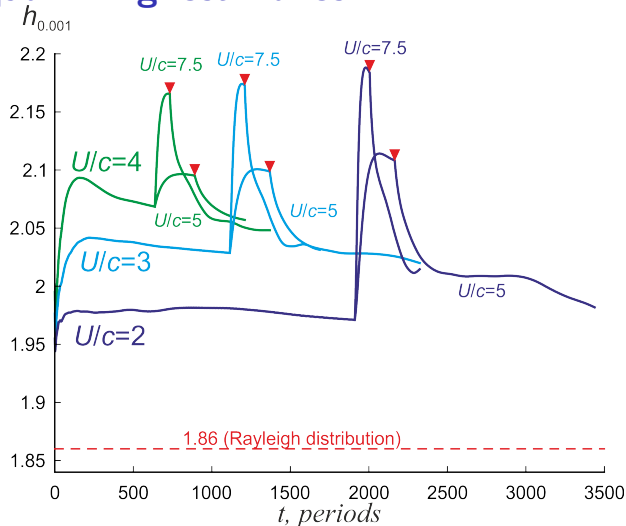
Evolution of the bound harmonics kurtosis  $C_4^{(b)}$ , initially under constant wind forcing with initial  $U/c_p = 2, 3, 4$ , then instantly increasing to 5 or 7.5 and decreasing back to the initial value. Red triangles mark end of squall

# squall - p.d.f.



Probability density function for wave heights, normalized by significant wave height: Rayleigh distribution (red curve), for  $U/c = 3$  at the start of the squall (blue curve), at the end of the squall with  $U/c = 7.5$  (green curve)

# Squall - highest waves



Maximum individual wave height with a probability of 0.001 (“highest wave in a thousand”) under constant wind forcing with initial  $U/c_p = 2, 3, 4$ , then instantly increasing to 5 or 7.5 and decreasing back to the initial value. Red triangles mark end of squall

## Conclusions

- ▶ Our model predicts that a squall significantly increases wave steepness and  $H_s$ . Surprisingly the Hasselmann eq-n does a good job, although the GKE is better able to describe fast changes and shows some new features.
- ▶ the GKE model yields both spectra and higher statistical moments, it can be efficiently computed with a fast parallel algorithm,
- ▶ within the framework of weakly nonlinear theory it is possible to find the PDF. Squall noticeably increases probability of rogue waves. The highest waves are most likely at the end of the squall.